



Rapid lateral flow immunoassay for the fluorescence detection of SARS-CoV-2 RNA

Daming Wang^{1,2,12}✉, Shaogui He^{3,12}, Xiaohui Wang⁴✉, Youqin Yan⁵, Jianzhong Liu⁵, Shimin Wu⁶, Shiguo Liu⁷, Yang Lei⁸, Min Chen⁹, Li Li⁹, Jieli Zhang⁸, Liwei Zhang⁸, Xiao Hu⁸, Xinhui Zheng⁸, Jiawei Bai⁸, Yulong Zhang⁴, Yitong Zhang¹⁰, Mingxuan Song² and Yuguo Tang^{1,11}✉

The coronavirus disease 2019 (COVID-19) pandemic has highlighted the need for rapid and accurate nucleic acid detection at the point of care. Here, we report an amplification-free nucleic acid immunoassay, implemented on a lateral flow strip, for the fluorescence detection of severe acute respiratory syndrome coronavirus 2 (SARS-CoV-2) RNA in less than one hour. The assay uses DNA probes that are designed to bind to the conserved open reading frame 1ab (ORF1ab), envelope protein (E) and the nucleocapsid (N) regions of the SARS-CoV-2 genome, and a fluorescent-nanoparticle-labelled monoclonal antibody that binds to double-stranded DNA-RNA hybrids. In a multi-hospital randomized double-blind trial involving 734 samples (593 throat swabs and 141 sputum) provided by 670 individuals, the assay achieved sensitivities of 100% and specificities of 99% for both types of sample (ground truth was determined using quantitative PCR with reverse transcription). The inexpensive amplification-free detection of SARS-CoV-2 RNA should facilitate the rapid diagnosis of COVID-19 at the point of care.

SARS-CoV-2 has spread globally to more than 100 countries and regions. Defined as SARS-CoV-2 by the International Committee on Taxonomy of Viruses, the enveloped virus belongs to the genus *Betacoronavirus*, and consists of round or oval particles with diameters ranging from 60 nm to 140 nm. On 11 January 2020, scientists published the whole-genome sequence of the novel coronavirus on the Virology Organization website (<https://virological.org/>). Two weeks later, after being approved by the National Medical Products Administration (NMPA), four nucleic acid detection kits for SARS-CoV-2 were released into the market. The genetic characteristics of this novel coronavirus are significantly different from the viruses that cause severe acute respiratory syndrome (SARS) and Middle East respiratory syndrome (MERS). Research has shown that SARS-CoV-2 has higher than 87.5% homology with bat SARS-like coronavirus (bat-SL-CoVZC45 and bat-SL-CoVZXC21)¹.

To discriminate between confirmed cases of COVID-19 and suspected cases, the aetiological diagnosis of novel-coronavirus pneumonia hinges mainly on molecular biological methods, such as nucleic acid detection and gene sequencing. Second-generation sequencing technology not only requires sophisticated equipment and skilled operators but it is also time-consuming and expensive. By contrast, nucleic acid detection methods may more easily meet clinical needs for diagnosis. Fluorescence-based quantitative PCR with reverse transcription (RT-qPCR) exhibits high sensitivity and specificity, yet turnaround times can be long (from hours to days), in part due to the need for nucleic acid purification and amplification. Moreover, nearly 60% of people infected with SARS-CoV-2 develop mild symptoms or no symptoms². There is therefore an urgent need

for the development of fast, simple and high-throughput assays for nucleic acid detection.

The application of the S9.6 monoclonal antibody with high affinity and selectivity to DNA-RNA hybrid molecules³ underlies the design of our method, which we name hybrid capture fluorescence immunoassay (HC-FIA). When presented with DNA-RNA heteropolymer duplexes prepared by transcription of ϕ X174 single-stranded DNA with DNA-dependent RNA polymerase³, this monoclonal antibody binds only to DNA-RNA hybrids and shows no response to single-stranded DNA, double-stranded DNA or ribosomal RNA. The capture of DNA-RNA hybrids by the S9.6 monoclonal antibody does not have sequence specificity³, and has been widely used in immunoprecipitation experiments of R-loop and DNA-RNA double-stranded hybrids⁴⁻⁶. Commercially available S9.6 antibodies have been used in diagnostic reagents for the human papilloma virus (HPV)⁷. The second generation of hybrid capture technology approved by the Food and Drug Administration can detect 13 high-risk HPV subtypes simultaneously⁸. The monoclonal antibody is also used to capture complexes formed by the hybridization of small RNA or microRNA, as well as various types of labelled DNA probes for signal conversion and amplification⁹⁻¹³.

In this Article, we used S9.6-monoclonal-antibody-labelled europium-chelate-based fluorescent nanoparticles (FNPs) to capture the hybridized double strands formed by the designed DNA probes and the RNA of SARS-CoV-2 on a lateral flow strip. Probe DNA-functionalized FNPs were used for signal amplification rather than target amplification, which provides substantial benefits with regard to workflows and the minimization of cross-contamination, consistent with the concept of point-of-care technology. The

¹Academy for Engineering & Technology, Fudan University, Shanghai, China. ²Suzhou Institute of Biomedical Engineering and Technology (SIBET), Chinese Academy of Sciences, Suzhou, China. ³Xiamen Huaxia University, Xiamen, China. ⁴Institute of Health Service and Transfusion Medicine, Beijing, China.

⁵Wuhan No. 7 Hospital, Wuhan, China. ⁶General Hospital of the Yangtze River Shipping, Wuhan, China. ⁷The Third People's Hospital of Hubei Province, Wuhan, China. ⁸Anbio (Xiamen) Biotechnology, Xiamen, China. ⁹Xiamen Center for Disease Control and Prevention, Xiamen, China. ¹⁰Department of Biochemistry and Molecular Biology, Harbin Medical University, Harbin, China. ¹¹CAS Key Laboratory of Biomedical Diagnostics, Chinese Academy of Sciences, Suzhou, China. ¹²These authors contributed equally: Daming Wang, Shaogui He. ✉e-mail: wangdm@sibet.ac.cn; lovechina1980@163.com; tangyg@sibet.ac.cn

HC-FIA has been developed into a commercial test kit for the diagnosis of SARS-CoV-2, and has recently been approved by the NMPA (registration number, 20203400298) and acquired the European Conformity (CE; registration number, NL-CA002-2020-50112) certification. A patent application has been submitted (application number, CN201811515744.1) and is presently under review¹⁴.

Results

In the HC-FIA system, probe DNA-functionalized FNP amplifies the signal of the hybridization of viral RNA and the DNA in the probe. The design principle of the HC-FIA biosensor is shown in Fig. 1.

Design and operation of the HC-FIA assay. The murine S9.6 monoclonal antibodies are prefixed onto the test line (T) of the lateral flow strip, and the control line (C) is coated with goat anti-rabbit IgG polyclonal antibodies (Fig. 1a). FNPs labelled with S9.6 antibodies and rabbit IgG are placed into the reaction tube. At the beginning of the detection process, the SARS-CoV-2 in the throat swab or sputum sample is lysed and released, and the released RNA hybridizes with the specific SARS-CoV-2 DNA probe. The resulting RNA–DNA hybrid is captured by the FNP-labelled S9.6 antibodies, and the complex flows along the sample pad and the nitrocellulose membrane towards the absorbent paper under capillary forces. When passing through the T area, the complex is captured by the S9.6 antibodies, gradually generating a fluorescent signal. In the C area, FNP-labelled rabbit IgG is captured by the anti-rabbit IgG. The presence or absence of the target SARS-CoV-2 RNA is based on a cut-off value for fluorescence intensity (Fig. 1b,c). Figure 1d shows a portable suitcase laboratory that has the ability to provide qualitative results in less than an hour after the following two steps: hybridization and immunofluorescence analysis (Fig. 1e).

Here we used the ratio of the test fluorescence signal to the control fluorescence signal (T/C) on the lateral flow strip such that the influence of any background fluorescence of the test card was minimized. By measuring the T/C ratio of throat swab samples from 211 healthy individuals, we found that the average background T/C ratio was 49.95, with a s.d. of 17.16 (Supplementary Fig. 1a). The receiver operating characteristic (ROC) curve and area under the curve (AUC) were used to determine the cut-off value and assess the diagnostic accuracy of the HC-FIA assay on the basis of sensitivity and specificity at various thresholds. We determined a ROC curve with an AUC of 0.999 with a 95% confidence interval (CI) of 0.997–1.000 (Supplementary Fig. 1b) using throat swab samples from 100 clinically confirmed and excluded COVID-19 cases. The cut-off value that obtained the highest sensitivity and specificity was determined to be 102.07, corresponding to the Youden index point of 0.980. Alternatively, a threshold value of twice the negative background value (here, $49.95 \times 2 = 99.90$) is usually used as the cut-off value in immunoassays. For convenience, we chose a T/C cut-off value of 100.00.

HC-FIA assay development. Optimization of DNA probes for the target RNA sequence of SARS-CoV-2 is key to improving assay efficiency. A list of all of the DNA probe sequences that we designed is provided in Supplementary Table 1. The genome of SARS-CoV-2 comprises approximately 30,000 bases, including a variable number (6–11) of open reading frames (ORFs). The first ORF accounts for about 67% of the entire genome, and encodes 16 non-structural proteins as well as helper proteins and structural proteins. The four main structural proteins are the spike glycoprotein (S), the small envelope protein (E), the matrix protein (M) and the nucleocapsid protein (N)^{15,16}. Most nucleic acid detection assays for SARS-CoV-2 use the following three conserved regions in the viral genome: ORF1ab, in which the RNA-dependent polymerase gene (*rdp*) is located¹⁵, and the regions that encode N and E.

We began by retrieving the RNA genome sequence of SARS-CoV-2 from the National Center for Biotechnology Information (NCBI) GenBank (accession numbers, [MN908947](#), [MN908947.3](#), [MN908947.2](#) and [NC_045512.1](#)). A detailed analysis of other published sequences for the SARS-CoV-2 genome revealed no notable variation in these regions. With the help of the design software Primer Premier 5.0, we designed three probes for each of the three regions: CoV01 and CoV04, located in the recommended region for the detection of ORF1ab and N, respectively; and CoV08, in the same region as E¹⁷. The genome positions of the probe binding sites in the reference genome sequence ([NC_045512.2](#)) are indicated in Fig. 1f.

Sequence alignment was conducted between the designed DNA probes and sequences from the human genome and from the genomes of viruses, bacteria, mycoplasma, chlamydia and other common pathogens. The probes matched the SARS-CoV-2 genomic sequence only, and we found no homology to human genomic DNA. Pseudoviruses carrying different regions of the target gene constructed using lentiviruses as vectors were used as positive controls. The target gene sequences of the pseudoviruses used are shown in Supplementary Table 2. P1 was positive for the SARS-CoV-2 N region, P2 for the SARS-CoV-2 E region and P3 for the SARS-CoV-2 ORF1ab region. The concentration of the three positive controls was 3,000 transduction units (TU) ml⁻¹, indicating that there were 3,000 infectious virus particles per ml. Physiological saline, purified water and pharyngeal swab samples positive for other common pathogens were used as negative controls of N1–N17. A list of information about the positive and negative references used in the study is provided in Supplementary Table 3. The test results are shown in Supplementary Tables 4–6. For the ORF1ab region, the probes CoV01 and CoV03 were selected; for the E region, the probe CoV08 was selected; and for the N region, the probes CoV04 and CoV06 preferentially bound to the target RNA. The selected DNA probes were further optimized by combination (Supplementary Table 7), with each group of probes simultaneously targeting all three segments. The HC-FIA test results in Supplementary Table 8 show that the combination of the CoV01, CoV04 and CoV08 probes (group 2) discriminated between all of the positive control samples and the negative controls, and detected positive samples with a low viral titre (1,000 TU ml⁻¹; Supplementary Table 3, L1–L3) at a positive rate of higher than 95%. Group 2 was therefore selected as the final combination. To date, there are 13,411 SARS-CoV-2 nucleotide sequences published on NCBI. Alignment of the three probes with the corresponding target region in the 13,411 uploaded sequences revealed that the target regions of the probes were conserved enough to yield 100% similarity.

We also optimized the testing conditions of the assay, in particular the incubation time for hybridization and the readout time of the test strip. The assay performance for incubation times of 10 min, 20 min, 30 min, 40 min, 50 min and 60 min at 56°C is shown in Supplementary Table 9. Note that 20 min was enough for the DNA probes to hybridize with the target region, which was reflected by the 100% positive rate in detecting positive throat swab and sputum samples with low viral titre (1,000 TU ml⁻¹; Supplementary Table 3, L1–L3). When the incubation time was extended to 50 or 60 min, the reaction was not as stable, as the positive rate of the L1–L3 reference samples decreased. Taking into consideration the detection efficiency and the requirement for virus inactivation, we selected 30 min as the incubation time for hybridization at 56°C. We also assessed the reading time of the strip for the values 10 min, 12 min, 15 min and 18 min (Supplementary Table 10). The results indicated that 12 min or longer led to the correct detection of the positive and negative reference samples. However, the coefficient of variation (CV) was lower than 10% for detecting positive samples with a low viral titre only when using a reading time of 15 min. We therefore selected a reading time of 15 min.

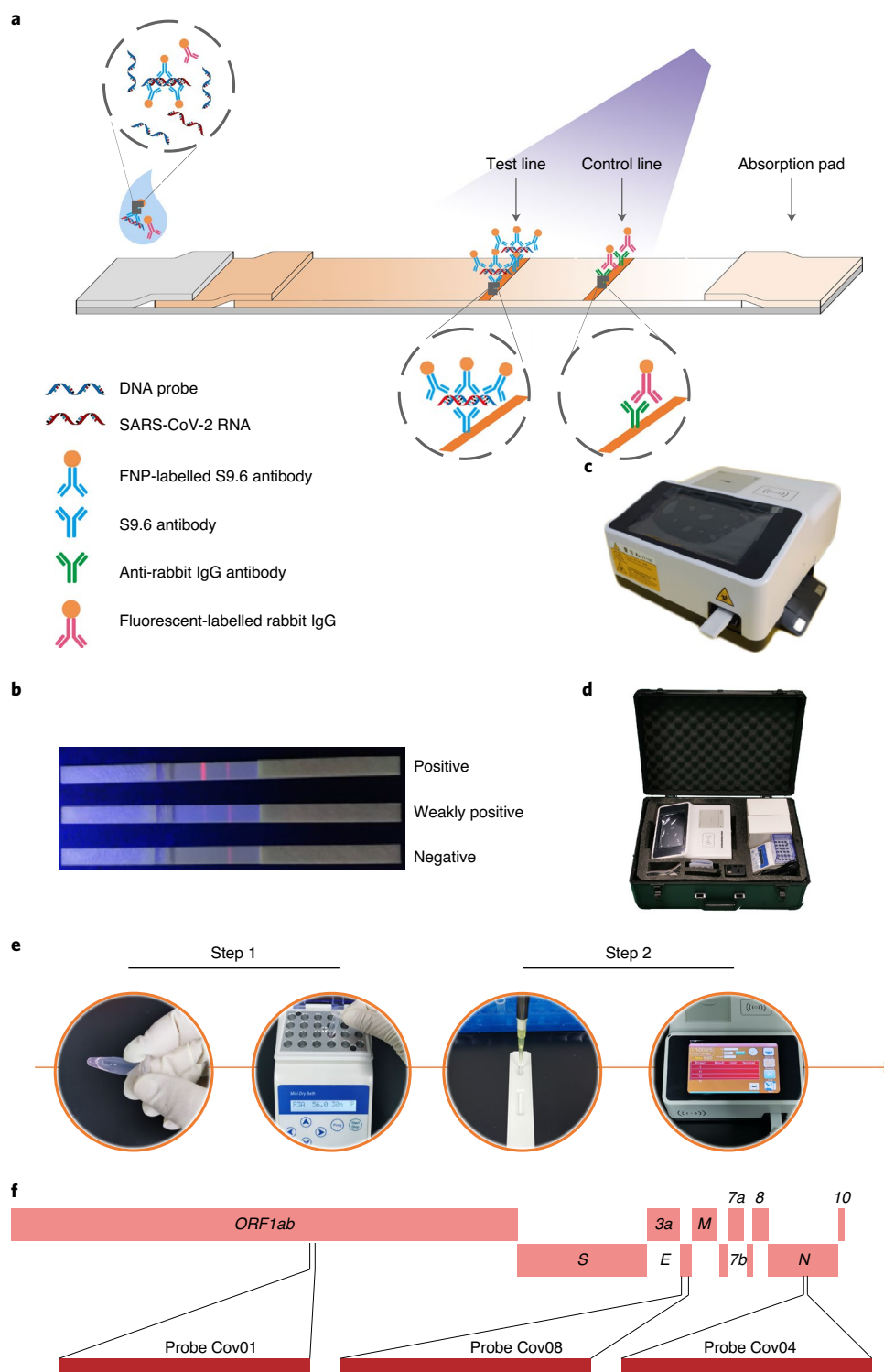


Fig. 1 | The SARS-CoV-2 HC-FIA detection system. a, The principle of HC-FIA. **b**, Representative results on a lateral flow strip. **c**, The fluorescence analysis device. **d**, A photograph of the portable suitcase laboratory, which has a length of 55.5 cm, a width of 37 cm and a height of 23 cm, with a weight of 8.5 kg. **e**, The testing process of the HC-FIA assay. Step 1: nucleic acid hybridization in an incubator at constant temperature. Step 2: determination of the intensity of the fluorescence signals on the test card using the device shown in c. **f**, Probe distribution in the genome of SARS-CoV-2.

Guanidinium thiocyanate and guanidine chloride—the most-used protein denaturants for nucleic acid extraction—were compared as transport media for sample preservation. Guanidinium thiocyanate led to better performance at discriminating between positive and negative samples, with a relatively low CV for samples with a low viral titre. In fact, guanidinium thiocyanate at a concen-

tration as high as 6 mol l^{-1} has shown excellent antiviral properties¹⁸. We selected guanidinium thiocyanate at a concentration of 5 mol l^{-1} as the protein denaturant for viral inactivation in transport medium.

Specificity of the HC-FIA assay. After optimizing the probe sequences and reaction conditions, we examined the specificity of

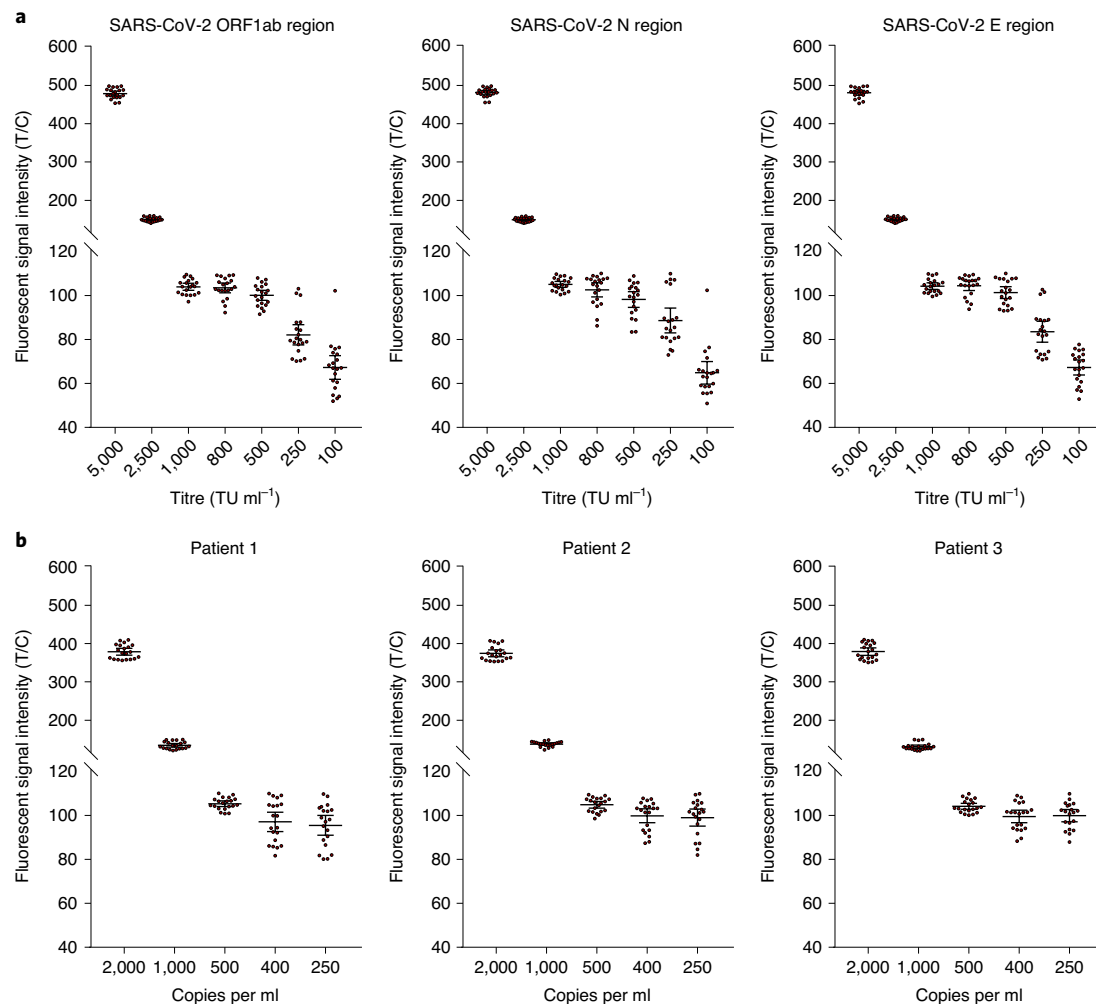


Fig. 2 | Sensitivity of the HC-FIA assay. The vertical axes show the fluorescence-intensity ratio (T/C) of the test signal (T) and the control signal (C). For each concentration, 20 tests were conducted in parallel. The LOD was determined as the concentration at which the positive rate was greater or equal to 95%. **a**, T/C ratios for serially diluted pseudovirus samples positive for the N, E and ORF1ab regions of SARS-CoV-2. **b**, T/C ratios for serially diluted throat swab samples from three critically ill patients. Data are mean \pm s.d.

the HC-FIA assay for detecting SARS-CoV-2. The positive controls included pseudoviruses (samples P1–P3) with target genes, and five clinical throat swab samples (samples P4–P8), confirmed using a RT-qPCR-based nucleic acid detection kit (Shanghai ZJ Bio-Tech). The negative controls, which consisted of throat swab samples, were confirmed to be negative for SARS-CoV-2, and positive for influenza A, influenza B, respiratory syncytial virus, chlamydia pneumoniae, adenovirus or other pathogens (samples N5–N17), or pseudovirus-positive for the N region of MERS (sample N18) or SARS (sample N19). A list of all of the samples is provided in Supplementary Table 3. A list of the detection results of 8 positive reference samples and 15 negative reference samples is provided in Supplementary Table 11.

We investigated whether there was cross-reactivity between SARS-CoV-2 and 55 common pathogens that cause respiratory diseases. The source and quantitative information of each pathogenic microorganism is provided in Supplementary Dataset 1. The original virus titre was determined to be 10^6 plaque-forming units per ml using a plaque assay. For interference samples of bacteria, mycoplasma and chlamydia, the concentration level was 10^7 colony-forming units per ml. Furthermore, human genomic DNA was extracted and quantified to be $90\text{--}105\mu\text{g ml}^{-1}$ from

three whole-blood samples. The HC-FIA assay exhibited excellent specificity for SARS-CoV-2, with no obvious cross-reactivity with all of the other pathogen samples and human genomic DNA (Supplementary Dataset 1).

As the monoclonal antibody S9.6 also binds to RNA–RNA duplexes¹⁹, especially AU-rich ones²⁰, we designed double-stranded RNA sequences with varying fractions of AU. Detailed sequence information is provided in Supplementary Table 12. As shown in Supplementary Table 13, regardless of AU content, the HC-FIA assay did not exhibit a detectable positive signal towards double-stranded RNA, which indicates that there is a low binding affinity between the S9.6 antibody and double-stranded RNA under the assay conditions. We also investigated whether the presence of double-stranded RNA affects the performance of the assay in the detection of clinical throat swab or sputum samples. We used 2 positive throat swab samples, 2 positive sputum samples, 10 negative throat swab samples and 5 negative sputum samples. We measured the T/C ratios with regard to the T/C values of the interference-free test, and found that the ratios ranged between 0.9 and 1.1 (Supplementary Dataset 1). This indicates that the presence of double-stranded RNA, regardless of AU content, does not significantly affect the performance of the HC-FIA assay.

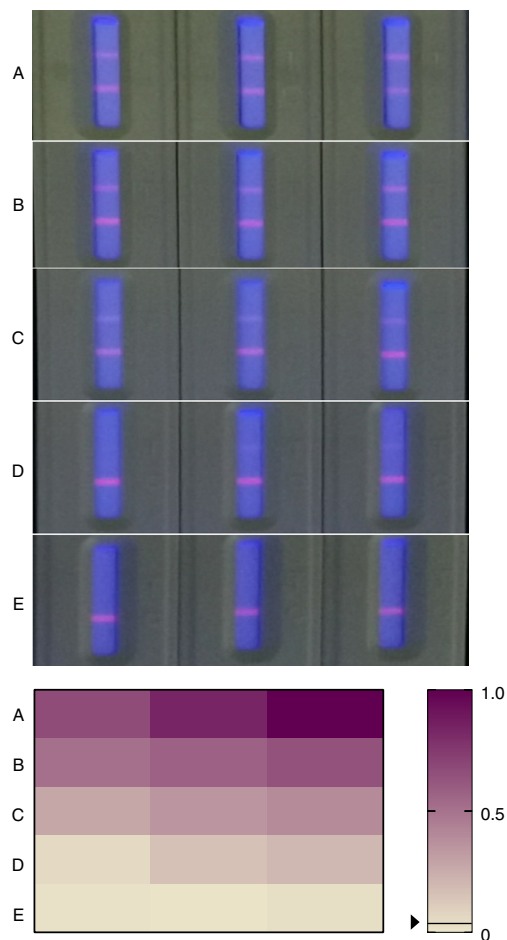


Fig. 3 | Visualization of the assay results. Photographs of typical results under a fluorescent light source, and the corresponding fluorescence readouts as a colour-gradient matrix, normalized to the maximum readout value. Group E consists of COVID-19-negative results only. The horizontal line on the colour bar indicates the cut-off value. A colour-gradient matrix for the fluorescence readouts of 734 clinical samples is provided in Supplementary Fig. 4, and the corresponding numerical data in Supplementary Dataset 3.

Sensitivity and precision of the HC-FIA assay. We serially diluted the pseudovirus samples containing three sections of target genes to titres of 5,000, 2,500, 1,000, 800, 500, 250 and 100 TU ml⁻¹, and calculated the average T/C values for 20 parallel tests. Figure 2a shows that the limit of detection (LOD) values of pseudovirus positive for the N, E or ORF1ab regions of SARS-CoV-2 were as low as 1,000 TU ml⁻¹, with a positive rate larger than 95%. When the titres of pseudovirus samples reached 10⁸ TU ml⁻¹, no notable hook effect was observed (Supplementary Fig. 2). The linear range of the assay corresponds to titres between 10³ and 10⁶ or 10⁷ TU ml⁻¹.

Throat swab samples from three critically ill patients—who were determined to be positive for SARS-CoV-2 using RT-qPCR, and the viral loads were quantified using digital PCR—were mixed with negative throat swab samples to prepare serial dilutions of 2,000, 1,000, 500, 400 and 250 copies per ml. As shown in Fig. 2b, the LOD was 500 copies per ml with a positive rate of higher than 95%. Clinical throat swab samples with T/C values close to the critical value (100) for positivity (samples with 512, 489 and 497 copies per ml of the ORF1ab region, according to digital PCR) were used to verify the LOD (tests performed 20 times in parallel). The positive rates of these samples were higher than 95% (Supplementary Tables 14–16).

Table 1 | Clinical diagnosis and outcomes of the RT-qPCR and HC-FIA assays for 670 cases and 734 samples

		HC-FIA		
		Positive	Negative	Total
Clinical diagnosis ^a	Confirmed cases	210	27	237
	Excluded cases	22	411	433
	Total	232	438	670
RT-qPCR ^b	Positive	249	0	249
	Negative	4	481	485
	Total	253	481	734

^aEach case was included only once. A case in which the individual had both sputum and throat swabs sampled simultaneously was included only in the sputum-sample group. ^bIf the first test gave an invalid result, the test was repeated and the invalid result was discarded.

To evaluate the precision of the HC-FIA kit, parallel tests were performed 20 times for each clinical throat swab sample for five consecutive days. The representative clinical samples chosen were a positive sample (1,348 copies per ml of the ORF1ab region), a sample from a critically ill individual (critical; 512 copies per ml) and a negative sample (0 copies per ml). The average T/C values of the three batches in detecting the positive sample were as follows: 199.92 ± 8.25 (CV = 4.13%), 200.68 ± 7.91 (CV = 3.94%) and 199.03 ± 7.43 (CV = 3.73%), respectively, compared with 109.17 ± 5.68 (CV = 4.65%), 110.80 ± 5.63 (CV = 5.08%) and 111.48 ± 4.67 (CV = 4.19%) for the critical sample, and with 44.66 ± 3.36 (CV = 7.52%), 43.99 ± 2.72 (CV = 6.18%) and 44.72 ± 2.98 (CV = 6.66%) for the negative sample. The batch-to-batch CV values were 3.89%, 4.66% and 6.74%. Thus, the assay showed good precision and reproducibility for the detection of SARS-CoV-2.

Robustness of the HC-FIA assay. To learn about the robustness of HC-FIA, we evaluated the effects of endogenous interference substances (such as haemoglobin and mucin) and of exogenous interference substances (in particular, clinical drugs commonly used in the treatment of patients with respiratory infections, including antiviral drugs, antibiotics and hormones). For this experiment, we used 18 clinical throat swab samples, including six critical samples (500–530 copies per ml for the ORF1ab region, according to digital PCR), six negative samples and six positive samples. The results were also recorded as the ratio of T/C values (interference samples versus control samples). In the prepared interference samples, haemoglobin concentrations were 0.5 g l⁻¹, 1.0 g l⁻¹ and 2.0 g l⁻¹, and the concentrations for mucin were 5 g l⁻¹, 10 g l⁻¹ and 20 g l⁻¹. The drug concentrations of exogenous interference samples (Supplementary Tables 17–19) were much higher than their peak plasma concentrations in vivo. As expected, all of the T/C ratios were in the range of 0.9–1.1 (Supplementary Dataset 2), indicating that the HC-FIA assay is robust to interference.

Clinical evaluation of the HC-FIA test kit. To further evaluate the performance of HC-FIA assay, a randomized double-blind clinical trial was performed by comparing the assay with RT-qPCR (SARS-CoV-2-detection kit produced by Shanghai ZJ Bio-Tech, and approved by NMPA) or with clinical diagnosis results in three independent medical institutions. The HC-FIA test kit used in the clinical evaluation contained test cards, lysis buffer, sample-preservation solution, positive and negative controls, and a reaction tube with DNA probes and labelled antibodies. The clinical diagnosis results of confirmed or excluded COVID-19 cases, which were provided by the designated hospitals, were based on computed tomography images and on the clinical manifestations of the patients, as specified by the guidelines of ‘Diagnosis and Treatment Protocol for

Table 2 | Performance of HC-FIA with respect to clinical diagnosis or RT-qPCR (as ground truths)

		Sensitivity		Specificity		Total consistency rate		κ
		Positive consistency rate (%)	95% CI (%)	Negative consistency rate (%)	95% CI (%)	Consistency rate (%)	95% CI (%)	
HC-FIA/clinical diagnosis	Throat swabs	87.69	83.08–92.30	95.01	92.82–97.20	92.53	90.38–94.68	0.8323
	Sputum	91.94	85.16–98.72	92.41	86.57–98.25	92.20	87.77–96.63	0.8419
	All samples	88.61	84.57–92.65	94.92	92.85–96.99	92.69	90.72–94.66	0.8393
HC-FIA/RT-qPCR	Throat swabs	100	99.85–100	99.26	98.43–100	99.49	98.92–100	0.9883
	Sputum	100	99.74–100	98.73	96.26–100	99.29	97.90–100	0.9856
	All samples	100	99.87–100	99.18	98.38–99.98	99.46	98.93–99.99	0.9879

Positive consistency rate = true positive (TP)/(TP + false negative (FN)); negative consistency rate = (true negative (TN))/(TN + false positive (FP)); total consistency rate = (TP + TN)/(TP + TN + FP + FN).

Novel Coronavirus Pneumonia (Trial Version 6.0)’ of China. A total of 734 samples (593 throat swabs and 141 sputum) provided by 670 individuals were tested in parallel. The raw data from the clinical trials are provided as Supplementary Dataset 3. The RT-qPCR detection kit that we used was designed as a three-target (ORF, N and E) system, and we followed the test–retest principle to discriminate between positive and negative samples. In addition to four failure tests caused by an invalid internal standard, eight retests were conducted: one because only one target *rdp* gene was positive, and seven because only the *N* and *E* genes were positive. In these cases, the previous negative results were excluded.

Of the 670 patients enrolled in the trial, 313 were male (46.72%) and 357 were female (53.28%). As shown in Supplementary Fig. 3, the age distribution of the enrolled population is similar to the age distribution of SARS-CoV-2 infection²¹. The visiting rate and diagnosis rate were also balanced. The results from the HC-FIA test kits are shown in Fig. 3, which shows photographs of typical results under a fluorescent light source and the corresponding gradient colour matrix after readout normalization. The gradient colour matrix in Supplementary Fig. 4 shows the normalized fluorescence readouts of 734 clinical samples (Supplementary Dataset 3).

For 621 cases, the HC-FIA results and the clinical diagnoses were consistent (210 confirmed cases and 411 excluded cases; Table 1); 49 cases (27 confirmed and 22 excluded by clinical diagnosis) were inconsistent with the HC-FIA results. For 730 samples, the results from the HC-FIA test were consistent with RT-qPCR (249 positive and 481 negative; Table 1). Four samples that were negative on the basis of RT-qPCR were positive using HC-FIA. Three of these samples were from patients who were clinically diagnosed as COVID-19-excluded, indicating that the HC-FIA test had given false-positive results. The remaining sample corresponded to a confirmed case by clinical diagnosis, in agreement with the HC-FIA test.

Cohen’s Kappa (κ), which is a frequently used metric of the reliability of agreement between categorical variables, is a more robust measure compared with simple percentage agreement between the variables, as κ takes into account agreements that occur by chance, especially in imbalanced datasets. We considered a κ value of greater than 0.75 to indicate a high level of agreement (perfect agreement corresponds to a $\kappa = 1$). As shown in Table 2, the results from the HC-FIA test were in high agreement with clinical diagnosis ($\kappa = 0.8393$) and with RT-qPCR ($\kappa > 0.98$, regardless of sample type).

Discussion

The HC-FIA assay has the potential to become a simpler alternative to RT-qPCR in the detection of SARS-CoV-2. The monoclonal antibody S9.6, which specifically recognizes DNA–RNA double-stranded hybrids, enables the use of immunofluorescence

for the detection of nucleic acids. Reading the T/C ratio of fluorescence values, rather than the absolute fluorescence values of the T line and the C line, improves the precision and reproducibility of the assay. We used a fluorescent reader and FNP (instead of optical readouts using colloidal gold-based test strips) for more accurate quantitative analyses.

Long DNA probes ensured high sensitivity and specificity.

When designing the DNA probe, we followed the general principles of PCR, such as a random distribution of bases, the generation of no secondary structures and no repeated DNA sequences. We used probes with a length of 40–120 bp (118, 99 and 89 bp for the CoV01, CoV04 and CoV08 probes, respectively); these are much longer than general PCR primers and TaqMan probes. This is due to the fact that long probes facilitate the formation of longer hybrids, thereby increasing the sensitivity of recognition by S9.6 (ref. ³). Despite the absence of nucleic acid amplification, the LOD of HC-FIA (500 copies per ml) is comparable to that of commercial RT-qPCR technology (200–1,000 copies per ml)²². The affinity of the S9.6 for DNA–RNA hybrids, the molar ratio of the monoclonal antibody to the hybrid and the efficiency of signal amplification are of critical importance for determining the sensitivity of the HC-FIA assay. The molar ratio of S9.6 to the RNA–DNA hybrid was documented to be 11–13 under certain conditions, suggesting that a hybrid can bind to more than a dozen antibodies, leading to signal amplification³. Moreover, the simultaneous three-DNA-probe system allows for more binding sites to be amplified. The HC-FIA assay appears to be more sensitive in detecting clinical samples than pseudoviruses (a LOD of 500 copies per ml for clinical throat swab samples, and a LOD of 1,000 TU ml^{−1} for pseudoviruses); however, we used three target genes for the clinical samples, and only a single target region for the pseudoviruses. Importantly, the ultralong probes in the HC-FIA assay completely match the conserved region of the target genes, ensuring the specificity of the assay (shorter primers and probes in RT-qPCR can cross-react with other coronaviruses, especially for the probes targeting the *N* and *E* genes). We confirmed the absence of any significant cross-reactivity between the long DNA probes and the RNA of other coronaviruses, such as SARS-CoV, MERS-CoV, coronavirus 229E and coronavirus OC43 (Supplementary Dataset 1). Thus, the assay is highly specific for SARS-CoV-2.

Further evidence of low or undetectable cross-reactivity is provided by the negative result of detecting rotavirus A (from ATCC, VR-2018), the genome of which consists of 11 segments of double-stranded RNA (Supplementary Dataset 1). As it has been shown using surface plasma resonance that the single-chain variable fragment of S9.6 has a binding affinity that is about 5× lower for AU-rich RNA–RNA hybrids compared with DNA–RNA hybrids

Table 3 | Attributes of the HC-FIA assay and a typical commercially available RT-qPCR kit for the detection of SARS-CoV-2 RNA

Principle	HC-FIA	RT-qPCR ³¹
Pretreatment	Amplification free	Nucleic acid extraction and purification
Assay time	Less than 1 h	2–3 h
Operating environment	On-site and on-demand detection	Requires specialized laboratories
Requirements for operator	No need for professional technicians Operators can be easily trained	Requires trained technicians
Equipment	Portable suitcase	Precision instruments, non-portable
Throughput	60 tests per hour ^a	96 tests per 4 h
Application scenarios	Outpatient departments, emergency departments, customs, disease-control sites	Central laboratories
Potential risk of pollution	No laboratory-contaminating product	Risk of contamination from amplicons

^aCalculated on the basis of the one-man operation of a single fluorescence-analysis device. Liquid transfer is the rate-limiting step for throughput improvement.

(for 23 bp hybrids), the high selectivity of the HC-FIA assay may be explained either by the high ionic conditions in the hybridization system (owing to the high salt preservation solution)¹⁹ or by the relative long DNA probes³, which may magnify variations in the binding affinity between AU-rich double-stranded RNA and DNA–RNA hybrids.

As saliva and sputum are mostly mucus, antibodies, lysozyme, inorganic salt and other protein or cell components (besides pathogenic microorganisms), we chose mucin—the major component of saliva—as a typical endogenous interference substance (besides haemoglobin) that could affect the robustness of the HC-FIA assay. We also evaluated drugs that are commonly used for respiratory diseases (which can make it into clinical samples). The design of the ultralong probes ensured that the assay has the ability to distinguish between SARS-CoV-2 and other infectious diseases and the presence of comorbidities. We attribute the robustness of the assay to the high affinity of the monoclonal antibody S9.6 to DNA–RNA hybrids, and to the optimized assay conditions.

Advantages of the HC-FIA assay. The HC-FIA assay does not need nucleic acid extraction, reverse transcription or nucleic acid amplification. The entire detection process involves only the following two steps: nucleic acid hybridization and immunofluorescence analysis (Fig. 1e and Supplementary Table 20). SARS-CoV-2 can be inactivated by incubation at 56 °C for 30 min, and the absence of nucleic acid amplification means that the assay does not suffer from contamination by amplicons. As shown in Supplementary Table 20, the materials needed for each test cost as little as US\$2. The portable device for reading the fluorescence signal can meet the demands of point-of-care technology. A list of the advantages of HC-FIA over RT-qPCR is shown in Table 3.

CRISPR-based assays on the basis of Cas13 or Cas12 endonucleases have also been developed using lateral flow technology^{23–27}. However, these assays require nucleic acid extraction and recombinase polymerase amplification or loop-mediated isothermal amplification. Assay times of CRISPR-based diagnostics and HC-FIA for the detection of SARS-CoV-2 are similar, yet the LOD values of the CRISPR-based diagnostics are higher (in the order of 10⁴–10⁵ copies per ml for SARS-CoV-2 (refs. ^{23,27}) and 1,000 copies per ml for the detection of the Zika virus and the dengue virus²⁵).

In summary, we present an amplification-free, inexpensive and rapid SARS-CoV-2 nucleic acid detection system that is amenable for point-of-care use. The assay—which involves detection reagents, an immunofluorescence lateral flow strip and a fluorescence-analysis device—is based on the capture of RNA–DNA hybrids and on immunofluorescence analysis. The assay and test kit could be adapted for the detection of other viral RNA.

Methods

Antibodies. The monoclonal antibody S9.6 (MABE1095, 3275033) used in the work was purchased from EMD Millipore. It was purified with protein G and was stored in buffer containing 0.1 M Tris-glycine (pH 7.4), 0.15 M NaCl with 0.05% sodium azide at 2–8 °C. Rabbit IgG (molecular mass, 150 kDa; AGRIG-0100, 021428216) and goat anti-rabbit IgG (molecular mass, 150 kDa; ABGAR-0500, 011530057) were purchased from Arista Biologicals and stored in pH 7.4 PBS at 2–8 °C; the former was purified by protein A from normal rabbit serum (purity ≥ 90%), while the latter was purified from whole goat antisera using immunoaffinity chromatography (purity ≥ 90%).

DNA probes and reagents. The DNA probes were synthesized by Biologo and purified using high-performance liquid chromatography (purity ≥ 95%). *N*-(3-dimethylaminopropyl)-*N*-ethylcarbodiimide hydrochloride (EDC, 25953-53-8), haemoglobin (9008-02-0) and mucin (114956-81-9) were purchased from Sigma-Aldrich. FNP composed of europium chelate (diameter, 210 nm) with a carboxylated surface were produced by Nanjing Microdetection Bio-Tech (MD20190831-1). Exogenous interference substances, namely drugs that might be used in treating patients with respiratory infections, are commercially available.

Pseudovirus production. The pseudoviruses, used as positive or negative references in the study, were provided by Sangon Biotech. The lentiviral vector system consisted of three plasmids of serial lentiviral vector (carrying target gene), psPAX2 vector and pMD2G vector according to the previously described method^{28,29}. pLV-CMV-MCS-EF-ZsGreen encoding the target sequence and ZsGreen was constructed by the provider. psPAX2 and pMD2G were obtained from Addgene. Pseudovirions were produced by cotransfection of HEK293T cells with psPAX2, pMD2G and pLV-CMV-MCS-EF-ZsGreen encoding the target sequence using calcium phosphate. Target RNA was transcribed, and the proteins were translated from psPAX2 and pMD2G. The RNA and protein were then packaged as lentiviruses. A list of information about the target gene sequences carried by pseudoviruses is provided in Supplementary Table 2. The titre of the obtained pseudovirus particles was determined by counting infected cells using fluorescence microscopy after serial dilution.

The source and quantitative information of the various pathogenic microorganisms used to determine the specificity of the assay are provided in Supplementary Dataset 1.

Labelling antibodies with FNPs. FNPs (1%) dispersed in deionized water (1.0 mg ml⁻¹) and EDC solution of 0.6 mg ml⁻¹ were added to 0.05 mol l⁻¹ boracic buffer (pH 8.0) on a rotary mixer for 20 min. The FNPs were separated by centrifugation at 15,000–16,000 r.p.m. for 30 min and resuspended in 0.05 mol l⁻¹ boracic acid buffer. The antibody solution at a final concentration of 0.2 mg ml⁻¹ was then added to the activated FNP solution, and the reaction system was placed onto a rotary mixer for 2 h. BSA solution (0.1 ml, 10%) was added to 1.0 ml FNP-labelled antibody solution for blocking, and the mixture was placed into a rotary mixer for 12–16 h. Finally, the FNP-labelled antibody solution was separated using centrifugation at 15,000–16,000 r.p.m. and washed twice with an equal volume of 0.05 mol l⁻¹ boracic acid buffer, and the as-prepared mixture was resuspended in the washing buffer to obtain FNP-labelled antibody solution.

Fluorescence analysis device. The supporting fluorescence analysis device (registration certificate, 20172400062) was made by Anbio (Xiamen) Biotechnology and is commercially available. It consists of a light-source system, a photoelectric detection system, a signal-amplifier circuit, a thermal printer and a

touch screen. It has a length of 22 cm, width of 23.6 cm and a depth of 9 cm, with a weight of approximately 3 kg.

HC-FIA test-kit workflow. The HC-FIA test kit was produced by Anbio (Xiamen) Biotechnology. The workflow complied strictly with the product manual. A list of the operation procedure, approximate cost of the materials needed and duration of the HC-FIA assay is provided in Supplementary Table 16. First, all of the reagents and specimens were prepared and equilibrated to room temperature before use. Reaction tubes were prepared according to sample quantity. Lysis buffer (85 µl) was added to each tube before the tube was shaken to mix the contents for the next step. We added 20 µl positive control, negative control or sample to the reaction tube. The control and sample tubes were then reversed three times and incubated at 56 °C in an incubator for 30 min. Next, 100 µl of the incubated sample was added to the test card sample well and left to rest for 15 min. The test card was inserted into the fluorescence analysis device, then the start button was pressed and the result was printed out. For quality control, a mixture of the three pseudoviruses (P1, P2 and P3 at a concentration of 2,000 TU ml⁻¹, carrying their target region of ORF1ab, N and E) was used as a positive control sample to ensure proper sample extraction and S9.6 binding, while physiological saline was used as a negative control. Before each new run of a test, the positive and negative controls should deliver an expected result to ensure the validity of the test result. If the control line was invalid, the analyser would display the text 'Error', indicating that the result of the test was invalid.

Clinical trial participants. The randomized double-blind clinical evaluation of HC-FIA SARS-CoV-2 kits was performed independently in three designated hospitals that were treating patients with COVID-19. This clinical trial was approved by the ethics committees for drug clinical trials of the three hospitals. The study was registered at <http://www.chictr.org> as ChiCTR2000033104, and was conducted by trained healthcare workers from the clinical institutions and our research team. As the samples used in the current trials were remnants after clinical nucleic acid detection, and double-blinded experimental design ensured the safety of patient privacy, waivers of the patients' informed consent were approved by the ethics committee. The case enrolment criteria referred to the guidelines of 'Diagnosis and Treatment Protocol for Novel Coronavirus Pneumonia (Trial Version 6.0)' of China.

Clinical evaluation. The HC-FIA SARS-CoV-2 kit was provided by Anbio (Xiamen) Biotechnology. The RT-qPCR detection kit for contrast research was produced by Shanghai ZJ Bio-Tech and used with an ABI 7500 Real-Time PCR System. First, the clinical information of the enrolled cases was collected, including the case number (ID number), age, gender, clinical diagnosis and sample collection time. The enrolled samples were randomly numbered using a random number generation tool before being arranged for testing in a random order. For both HC-FIA and RT-qPCR, detection was repeated if the positive or negative control sample did not deliver the expected result. As for RT-qPCR, retests were conducted and the previous result was eliminated if only one channel or two channels (N and E) tested positive. If the retesting result corresponding to the *rdrp* gene remained positive, it was considered to be positive. By contrast, if only the channel associated with the N gene or/and the E gene was positive, the result might have been due to other coronaviruses and was regarded as negative. A total of 734 samples from 670 individuals were evaluated in parallel, including 593 throat swab samples and 141 sputum samples. The related clinical diagnosis results were provided by the hospitals according to the results of computed tomography images and the clinical manifestations of the patients.

Statistical analyses. ROC curves and AUC values were used to determine the cut-off value and assess diagnostic accuracy of the HC-FIA assay using SPSS v.19.0 software. For the consistency analysis between the HC-FIA and RT-qPCR or clinical diagnosis, Cohen's κ statistic was used in the comparison. A κ coefficient of less than 0.40 would suggest that the two methods are mutually inconsistent; a κ coefficient ranging from 0.40 to 0.75 indicates moderate agreement; and a κ coefficient of greater than 0.75 indicates high consistency. Two-tailed Mann-Whitney *U*-tests were performed to examine the significance of using the κ coefficient. Results are presented as mean \pm s.d.

Reporting Summary. Further information on research design is available in the Nature Research Reporting Summary linked to this article.

Data availability

The main data supporting the results in this study are available within the paper and its Supplementary Information. All data generated in this study, including source data and the data used to generate the figures, are available at Figshare (<https://doi.org/10.6084/m9.figshare.13102895>)³⁰.

Received: 16 May 2020; Accepted: 3 November 2020;

Published online: 3 December 2020

References

- Chen, L. et al. RNA based mNGS approach identifies a novel human coronavirus from two individual pneumonia cases in 2019 Wuhan outbreak. *Emerg. Microbes Infect.* **9**, 313–319 (2020).
- Qiu, J. Covert coronavirus infections could be seeding new outbreaks. *Nature* <https://doi.org/10.1038/d41586-020-00822-x> (2020).
- Boguslawski, S. J. et al. Characterization of monoclonal antibody to DNA • RNA and its application to immunodetection of hybrids. *J. Immunol. Methods* **89**, 123–130 (1986).
- Yan, Q., Shields, E. J., Bonasio, R. & Sarma, K. Mapping native R-Loops genome-wide using a targeted nuclease approach. *Cell Rep.* **29**, 1369–1380 (2019).
- Paull, T. T. RNA-DNA hybrids and the convergence with DNA repair. *Crit. Rev. Biochem. Mol.* **54**, 371–384 (2019).
- Toubiana, S. & Selig, S. DNA:RNA hybrids at telomeres—when it is better to be out of the (R) loop. *FEBS J.* **285**, 2552–2566 (2018).
- Ding, S. et al. Establishment of immunoassay for detecting HPV16 E6 and E7 RNA. *Sci. Rep.* **5**, 13686 (2006).
- Poljak, M. & Kocjan, B. J. Commercially available assays for multiplex detection of alpha human papillomaviruses. *Expert Rev. Anti Infect. Ther.* **8**, 1139–1162 (2010).
- Hu, Z., Zhang, A. & Storz, G. An antibody-based microarray assay for small RNA detection. *Nucleic Acid Res.* **34**, e52 (2006).
- Sipova, H. et al. Surface plasmon resonance biosensor for rapid label-free detection of microribonucleic acid at subfemtomole level. *Anal. Chem.* **82**, 10110–10115 (2010).
- Qavi, A. J., Kindt, J. T., Gleeson, M. A. & Bailey, R. C. Anti-DNA:RNA antibodies and silicon photonic microring resonators: increased sensitivity for multiplexed microRNA detection. *Anal. Chem.* **83**, 5949–5956 (2011).
- Tran, H. V., Piro, B., Reisberg, S., Duc, H. T. & Pham, M. C. Antibodies directed to RNA/DNA hybrids: an electrochemical immunosensor for microRNAs detection using graphene-composite electrodes. *Anal. Chem.* **85**, 8469–8474 (2013).
- Sguassero, A. et al. A simple and universal enzyme-free approach for the detection of multiple microRNAs using a single nanostructured enhancer of surface plasmon resonance imaging. *Anal. Bioanal. Chem.* **411**, 1873–1884 (2019).
- Wang, D. et al. Nucleic acid hybrid capture immunofluorescence detection method, immunofluorescence chromatography test strip and kit. Patent CN201811515744.1 (2018).
- Lu, R. et al. Genomic characterization and epidemiology of 2019 novel coronavirus: implications for virus origins and receptor binding. *Lancet* **395**, 565–574 (2020).
- Chan, J. F. et al. Genomic characterization of the 2019 novel human-pathogenic coronavirus isolated from a patient with a typical pneumonia after visiting Wuhan. *Emerg. Microbes Infect.* **9**, 221–236 (2020).
- Corman, V. M. et al. Detection of 2019 novel coronavirus (2019-nCoV) by real-time RT-PCR. *Euro Surveill.* **25**, <https://doi.org/10.2807/1560-7917.ES.2020.25.3.2000045> (2020).
- Roberts, P. L. & Lloyd, D. Virus inactivation by protein denaturants used in affinity chromatography. *Biologicals* **35**, 343–347 (2007).
- Kinney, J. S., Viscidi, R. P., Vonderfecht, S. L., Eiden, J. J. & Yolken, R. H. Monoclonal antibody assay for detection of double-stranded RNA and application for detection of group A and non-group A rotaviruses. *J. Clin. Microbiol.* **27**, 6–12 (1989).
- Phillips, D. D. et al. The sub-nanomolar binding of DNA-RNA hybrids by the single chain Fv fragment of antibody S9.6. *J. Mol. Recognit.* **26**, 376–381 (2013).
- Zhao, J. et al. Relationship between the ABO blood group and the COVID-19 susceptibility. *Clin. Infect. Dis.* <https://doi.org/10.1093/cid/ciaa1150> (2020).
- Wang, X. D., Shi, J., Ding, W. F., Jv, S. Q. & Zhao, J. H. Research state and application of new 2019 novel coronavirus nucleic acid detection. *Chin. J. Clin. Lab. Sci.* **38**, 81–84 (2020).
- Abudayyeh, O., Gootenberg, J. & Zhang, F. Enabling Coronavirus Detection Using CRISPR-Cas13: An Open-Access SHERLOCK Research Protocol (2020); <https://mcgovern.mit.edu/2020/02/14/enabling-coronavirus-detection-using-crispr-cas13-an-open-access-sherlock-research-protocol/>
- Myhrvold, C., Freije, C. A. & Gootenberg, J. S. Field-deployable viral diagnostics using CRISPR-Cas13. *Science* **360**, 444–448 (2018).
- Freije, C. A. et al. Programmable inhibition and detection of RNA viruses using Cas13. *Mol. Cell* **76**, 826–837 (2019).
- Kellner, M. J., Koob, J. G., Gootenberg, J. S., Abudayyeh, O. O. & Zhang, F. SHERLOCK: nucleic acid detection with CRISPR nucleases. *Nat. Protoc.* **14**, 2986–3012 (2019).
- Broughton, J. P. et al. CRISPR-Cas12-based detection of SARS-CoV-2. *Nat. Biotechnol.* <https://doi.org/10.1038/s41587-020-0513-4> (2020).
- Naldini, L., Blomer, U., Gage, F. H., Trono, D. & Verma, I. M. Efficient transfer, integration, and sustained long-term expression of the transgene in

- adult rat brains injected with a lentiviral vector. *Proc. Natl Acad. Sci. USA* **93**, 11382–11388 (1996).
29. Yang, Z. Y. et al. Evasion of antibody neutralization in emerging severe acute respiratory syndrome coronaviruses. *Proc. Natl Acad. Sci. USA* **102**, 797–801 (2005).
30. Wang, D. et al. Dataset for Rapid lateral flow immunoassay for the fluorescence detection of SARS-CoV-2 RNA. *Figshare* <https://doi.org/10.6084/m9.figshare.13102895> (2020).
31. Xie, C., Wu, H., Ma, X. & Zhou, G. New molecular diagnostic technologies for clinical detection of SARS-CoV-2. *Hereditas* **42**, 870–881 (2020).

Acknowledgements

We thank J. Wang for help in plotting the graphs. The work was funded by a National Key Research and Development Project (no. 2020YFC0847100).

Author contributions

D.W. conceived the research, ran the experiments and prepared the manuscript. Y.T. supervised all aspects of the work and gave guidance. X.W. and S.H. helped to design the clinical trials, drafted the manuscript and contributed to data analysis. Y.Y., J.L., S.W., S.L., M.C. and L.L. collected clinical samples from patients and participated in the clinical evaluation. Y.L., J.Z., L.Z. and X.H. performed experiments as well as clinical trials and analysed the raw data. X.Z. and J.B. participated in the statistical analyses.

Yulong Zhang contributed to plotting the graphs. Yitong Zhang provided assistance in probe design. M.S. provided advice on the design of the analysis device. All of the authors read, edited and approved the manuscript.

Competing interests

D.W., X.H. and L.Z. have submitted a patent application that is related to this work (application number, CN201811515744.1). The other authors declare no competing interests.

Additional information

Supplementary information is available for this paper at <https://doi.org/10.1038/s41551-020-00655-z>.

Peer review information: *Nature Biomedical Engineering* thanks Nongyue He and the other, anonymous, reviewer(s) for their contribution to the peer review of this work.

Correspondence and requests for materials should be addressed to D.W., X.W. or Y.T.

Reprints and permissions information is available at www.nature.com/reprints.

Publisher's note Springer Nature remains neutral with regard to jurisdictional claims in published maps and institutional affiliations.

© The Author(s), under exclusive licence to Springer Nature Limited 2020

Reporting Summary

Nature Research wishes to improve the reproducibility of the work that we publish. This form provides structure for consistency and transparency in reporting. For further information on Nature Research policies, see our [Editorial Policies](#) and the [Editorial Policy Checklist](#).

Statistics

For all statistical analyses, confirm that the following items are present in the figure legend, table legend, main text, or Methods section.

n/a Confirmed

- | | | |
|-------------------------------------|-------------------------------------|--|
| <input type="checkbox"/> | <input checked="" type="checkbox"/> | The exact sample size (n) for each experimental group/condition, given as a discrete number and unit of measurement |
| <input type="checkbox"/> | <input checked="" type="checkbox"/> | A statement on whether measurements were taken from distinct samples or whether the same sample was measured repeatedly |
| <input type="checkbox"/> | <input checked="" type="checkbox"/> | The statistical test(s) used AND whether they are one- or two-sided
<i>Only common tests should be described solely by name; describe more complex techniques in the Methods section.</i> |
| <input checked="" type="checkbox"/> | <input type="checkbox"/> | A description of all covariates tested |
| <input checked="" type="checkbox"/> | <input type="checkbox"/> | A description of any assumptions or corrections, such as tests of normality and adjustment for multiple comparisons |
| <input type="checkbox"/> | <input checked="" type="checkbox"/> | A full description of the statistical parameters including central tendency (e.g. means) or other basic estimates (e.g. regression coefficient) AND variation (e.g. standard deviation) or associated estimates of uncertainty (e.g. confidence intervals) |
| <input type="checkbox"/> | <input checked="" type="checkbox"/> | For null hypothesis testing, the test statistic (e.g. F , t , r) with confidence intervals, effect sizes, degrees of freedom and P value noted
<i>Give P values as exact values whenever suitable.</i> |
| <input checked="" type="checkbox"/> | <input type="checkbox"/> | For Bayesian analysis, information on the choice of priors and Markov chain Monte Carlo settings |
| <input checked="" type="checkbox"/> | <input type="checkbox"/> | For hierarchical and complex designs, identification of the appropriate level for tests and full reporting of outcomes |
| <input checked="" type="checkbox"/> | <input type="checkbox"/> | Estimates of effect sizes (e.g. Cohen's d , Pearson's r), indicating how they were calculated |

Our web collection on [statistics for biologists](#) contains articles on many of the points above.

Software and code

Policy information about [availability of computer code](#)

Data collection A fluorescence-analysis device (registration Certificate No. 20172400062) was employed to read out the signal on the lateral-flow dipstick.

Data analysis For statistical analyses of ROC curve and Kappa coefficients, we used SPSS Version 19.0. Data analyses and illustrations were done using Microsoft Excel 2010, GraphPad Prism Version 7.00 and Origin 85.

For manuscripts utilizing custom algorithms or software that are central to the research but not yet described in published literature, software must be made available to editors and reviewers. We strongly encourage code deposition in a community repository (e.g. GitHub). See the Nature Research [guidelines for submitting code & software](#) for further information.

Data

Policy information about [availability of data](#)

All manuscripts must include a [data availability statement](#). This statement should provide the following information, where applicable:

- Accession codes, unique identifiers, or web links for publicly available datasets
- A list of figures that have associated raw data
- A description of any restrictions on data availability

The main data supporting the results in this study are available within the paper and its Supplementary Information. All data generated in this study, including source data and the data used to make the figures, are available from figshare with the identifier <https://doi.org/10.6084/m9.figshare.13102985>.

Field-specific reporting

Please select the one below that is the best fit for your research. If you are not sure, read the appropriate sections before making your selection.

☒ Life sciences ☐ Behavioural & social sciences ☐ Ecological, evolutionary & environmental sciences

For a reference copy of the document with all sections, see [nature.com/documents/nr-reporting-summary-flat.pdf](https://www.nature.com/documents/nr-reporting-summary-flat.pdf)

Life sciences study design

All studies must disclose on these points even when the disclosure is negative.

Sample size	Sample sizes were determined according to "Key points of technical review of 2019 novel coronavirus nucleic acid detection reagent registration" promulgated by Center for Medical Device Evaluation of China in Feb. 12th, 2020. 20 parallel tests of each concentration were conducted for the determination of the limit of detection. 20 parallel tests for each clinical throat-swab sample were performed in 5 consecutive days. For the clinical trials, more than 200 confirmed cases and 300 excluded cases were included.
Data exclusions	If the internal reference failed for RT-qPCR or HC-FIA, retest was conducted with the first result eliminated. For some special cases in the clinical trials, namely a later confirmed case with previous negative results based on RT-qPCR, the negative results were eliminated. When only the N gene and the E gene were positive or only one channel was positive according to RT-qPCR, retest was conducted by RT-qPCR and the previous result was excluded.
Replication	All experiments have biological replicates.
Randomization	Before testing, the samples were randomly numbered. They were then tested in consecutive order.
Blinding	A randomized double-blind clinical evaluation of HC-FIA was performed. The samples were blind to the operator, and after being detected by RT-qPCR and HC-FIA, the results were recorded and matched according to the randomly assigned number.

Reporting for specific materials, systems and methods

We require information from authors about some types of materials, experimental systems and methods used in many studies. Here, indicate whether each material, system or method listed is relevant to your study. If you are not sure if a list item applies to your research, read the appropriate section before selecting a response.

Materials & experimental systems

n/a	Involved in the study
<input type="checkbox"/>	<input checked="" type="checkbox"/> Antibodies
<input checked="" type="checkbox"/>	<input type="checkbox"/> Eukaryotic cell lines
<input checked="" type="checkbox"/>	<input type="checkbox"/> Palaeontology and archaeology
<input checked="" type="checkbox"/>	<input type="checkbox"/> Animals and other organisms
<input type="checkbox"/>	<input checked="" type="checkbox"/> Human research participants
<input type="checkbox"/>	<input checked="" type="checkbox"/> Clinical data
<input checked="" type="checkbox"/>	<input type="checkbox"/> Dual use research of concern

Methods

n/a	Involved in the study
<input checked="" type="checkbox"/>	<input type="checkbox"/> ChIP-seq
<input checked="" type="checkbox"/>	<input type="checkbox"/> Flow cytometry
<input checked="" type="checkbox"/>	<input type="checkbox"/> MRI-based neuroimaging

Antibodies

Antibodies used	The monoclonal antibody S9.6 (Cat. # MABE1095, Lot # 3275033) was purchased from EMD Millipore Corporation (USA). Rabbit IgG (Product No. AGRIG-0100, Lot No. 021428216) and goat anti-rabbit IgG (Product No. ABGAR-0500, Lot No. 011530057) were purchased from Arista Biologicals Inc. (USA) and stored in pH 7.4 phosphate buffered saline at 2–8 °C.
Validation	The commercially available antibody clones used in this work are routinely employed for similar purposes in other test kits. Each lot used in this work had certificates of analysis from the manufacturers.

Human research participants

Policy information about [studies involving human research participants](#)

Population characteristics	670 subjects enrolled in the clinical evaluation of the HC-FIA assay referred to the guidelines for "Diagnosis and treatment of novel coronavirus infection pneumonia (Trial Version 6.0)" of China. The enrolled population shared the demographic characteristics of SARS-CoV-2 infection according to different age groups.
Recruitment	All the samples were provided by the clinical institutions. Since the samples used in the current trials were remnants after

Recruitment

clinical nucleic acid detection, and the double-blinded experimental design ensured patient privacy, waivers of the patients' informed consent were approved by the ethics committee.

Ethics oversight

The clinical-trial protocol was approved by the ethics committees for drug clinical trials of the three designated hospitals of COVID-19 in Wuhan.

Note that full information on the approval of the study protocol must also be provided in the manuscript.

Clinical data

Policy information about [clinical studies](#)

All manuscripts should comply with the ICMJE [guidelines for publication of clinical research](#) and a completed [CONSORT checklist](#) must be included with all submissions.

Clinical trial registration

The clinical trial has been registered on chictr.org (ChiCTR2000033104).

Study protocol

We used a randomized double-blind design to evaluate the performance of HC-FIA by comparing with RT-qPCR or clinical-diagnosis results in three independent medical institutions. The case enrollment criteria referred to "Diagnosis and treatment of novel coronavirus infection pneumonia (Trial Version 6.0)" of China. Parallel experiments were conducted on the same blinded samples by RTqPCR and HC-FIA.

Data collection

The throat-swab and sputum samples were collected from Feb. 18 to Mar 9, 2020 in the three designated hospitals of COVID-19 in Wuhan, where the clinical trials were carried out. The clinical-information data, including age, gender as well as results of the clinical diagnosis, were provided by the hospitals. The raw data of RT-qPCR and HC-FIA detection were simultaneously recorded by the operators in a double-blinded fashion.

Outcomes

The primary outcome was consistency between the results of the HC-FIA test and RT-qPCR or clinical diagnosis. Cohen's Kappa statistics were adopted to evaluate the consistency. A kappa coefficient in the range of 0.40–0.75 was assumed to indicate 'moderate agreement', whereas a kappa coefficient greater than 0.75 indicated 'high consistency'. Secondary outcomes were sensitivity and specificity of the HC-FIA assay in detecting SARS-CoV-2 in the clinical throat-swab and sputum samples.